APPLIED PHYSICS LETTERS 107, 234101 (2015)

Insights on proximity effect and multiphoton induced luminescence from gold nanospheres in far field optical microscopy

Johan Borglin,[1,2] Stina Guldbrand,[2] Hanne Evenbratt,[3,a)] Vladimir Kirejev,[1] Henrik Grönbeck,[4] and Marica B. Ericson[1,b)]

[1]*Biomedical Photonics Group, Department of Chemistry and Molecular Biology, University of Gothenburg, Kemivägen 10, 412 96 Gothenburg, Sweden*
[2]*Department of Physics, University of Gothenburg, Kemivägen 10, 412 96 Gothenburg, Sweden*
[3]*Pharmaceutical Technology, Department of Chemistry and Chemical Engineering, Chalmers University of Technology, Kemigården 4, 412 96 Gothenburg, Sweden*
[4]*Department of Applied Physics, Chalmers University of Technology, Kemivägen 9, 412 96 Gothenburg, Sweden*

(Received 25 June 2015; accepted 12 November 2015; published online 8 December 2015)

Gold nanoparticles can be visualized in far-field multiphoton laser-scanning microscopy (MPM) based on the phenomena of multiphoton induced luminescence (MIL). This is of interest for biomedical applications, e.g., for cancer diagnostics, as MPM allows for working in the near-infrared (NIR) optical window of tissue. It is well known that the aggregation of particles causes a redshift of the plasmon resonance, but its implications for MIL applying far-field MPM should be further exploited. Here, we explore MIL from 10 nm gold nanospheres that are chemically deposited on glass substrates in controlled coverage gradients using MPM operating in NIR range. The substrates enable studies of MIL as a function of inter-particle distance and clustering. It was shown that MIL was only detected from areas on the substrates where the particle spacing was less than one particle diameter, or where the particles have aggregated. The results are interpreted in the context that the underlying physical phenomenon of MIL is a sequential two-photon absorption process, where the first event is driven by the plasmon resonance. It is evident that gold nanospheres in this size range have to be closely spaced or clustered to exhibit detectable MIL using far-field MPM operating in the NIR region.
[http://dx.doi.org/10.1063/1.4936554]

Gold nanoparticles have been explored within biological research for more than a decade.[1] They demonstrate potential for a great variety of applications. Initially, gold nanoparticles were introduced as immunolabeling contrast for transmission and scanning electron microscopy (SEM).[2,3] Later, the unique optical properties and high biocompatibility of gold nanoparticles have stimulated interest within the biomedical optics field as contrast agent in connection to optical imaging modalities,[4–8] with the potential facilitate multimodal optical imaging. Multiphoton microscopy (MPM) is a far-field laser scanning optical microscopy technique, enabling high resolution non-invasive imaging of biological tissue applied for, e.g., non-invasive cancer diagnostics;[9,10] however, improved contrast mechanisms are required to fully take advantage of the method. In this respect, gold nanoparticles are interesting, given their ability to exhibit multiphoton induced luminescence (MIL, a.k.a. multiphoton absorption induced luminescence MAIL) upon irradiation of fs-pulsed near-infrared (NIR) laser light.[5,6,8,11–15] The combination of MIL and MPM has a unique potential for non-invasive optical nanoplasmonic sensing *in vivo*. This is a direction that has been recently demonstrated to have a great potential in the biomedical field.[16]

MIL from gold was described already in 1986, as an blue-shifted emission obtained from roughened gold surfaces when irradiated by NIR light.[17] As the emission was not observed from smooth gold surfaces, MIL was ascribed to be related to the nanostructure of the surface. The physical origin of MIL has been attributed to a sequential absorption of multiple photons,[12,13] which should not be confused with the coherent two-photon excitation exhibited by organic fluorophores generally utilized in MPM. It is generally accepted that gold nanorods exhibit substantially stronger luminescence signal compared to gold nanospheres (AuNSs).[12,18,19] The strong MIL from gold nanorods can be utilized for non-invasive imaging *in vivo*, but is not suitable for selective optical sensing as unspecifically bound particles in tissue will increase the background and obscure the signal. Thus, means for being able to tune the MIL emission should be explored, particularly in connection to far-field laser scanning optical microscopy, in order to develop protocols allowing for *in vivo* optical sensing.

It is well known that AuNSs in close proximity will redshift the surface plasmon resonance peak in the absorption spectra by acting together as a dipole.[20–22] It has been demonstrated that the generation of MIL is also affected by field-enhancement by varying the spacing between spherical particles,[15,23] implying that aggregates of AuNSs exhibit stronger MIL signal compared to individual particles. However, further understanding is required, particularly in the context

[a)]H. Evenbratt is presently (but not at the time of experiments) associated with Cline Scientific AB.
[b)]Author to whom correspondence should be addressed. Electronic mail: marica.ericson@chem.gu.se. Tel.: +46 31 786 9030.

of biomedical applications in combination with far-field MPM. In addition, there are recent reports claiming detection of MIL from AuNSs at the single particle level.[24–27] Recent results in our lab demonstrate that well-dispersed polyethylene glycol (PEG) coated spherical gold nanoparticles (AuNPs) with diameter less than 40 nm do not exhibit MIL in water solution using excitation powers relevant to biological experiments (unpublished data). Instead, MIL could only be detected when the spherical AuNPs were deposited on glass-coverslips. This led to the question whether or not MIL can be obtained from well-dispersed spherical particles at biologically relevant conditions using far-field optical microscopy, or if aggregation and clustering of the particles are necessary.

In this letter, we explore MIL from commercially available substrates (Cline Scientific AB, Gothenburg, Sweden) comprising 10 nm AuNSs created by chemical reduction using citrate and thereafter deposited on glass surfaces, forming controlled particle concentration gradients[28,29] (Figure 1(a)). These AuNS gradient substrates, originally designed for cell culturing experiments, were implemented here as a suitable model for methodical studies of MIL from deposited particles.[30] Figures 1(b) and 1(c) demonstrate the MIL emission acquired along a gradient plate using a commercial MPM-set up (LSM 710 NLO, Carl Zeiss MicroImaging GmbH, Germany) equipped with a Mai Tai DeepSee tunable NIR Ti:Sapphire fs-laser (Spectra-Physics, Newport Corporation, USA). SEM images (included in Figure 1(b)) illustrate the particle distribution at different locations along the gradient-plate. The particle coverage was assessed from the SEM images and represented as ratio of projected area using MatLab (Mathworks, Inc., Natick, MA, USA). In addition, inter-particle distance and cluster size were assessed from the SEM images. As seen from the figure, the emission signal is strongly correlated with the particle coverage. The intensity of the luminescence deviates from a linear dependency (Figure 1(c)), validated by a log-log analysis.[30] The non-linear dependence is particularly evident for coverage above 20%, corresponding to regions where cluster formation is present. Further AFM analysis confirmed that the observed effect can be attributed to the formation of clusters, rather than a simple volume effect.[30] This implies a non-linear enhancement of the emission as the inter-particle distance becomes smaller and the degree of clustering increases, supported by earlier reports.[14,15]

Absorption spectra (Figure 2(a)) of the substrates were obtained using a Varian Cary Eclipse 5000 (Varian, Inc., USA) spectrophotometer at two different locations corresponding to areas with particle coverage of approximately 15 and 30%. All spectra demonstrate the characteristic surface plasmon resonance peak located at 520 nm, corresponding to AuNSs of 10 nm size.[31] The increased absorption in the NIR region acquired for areas corresponding to 30% particle coverage is attributed to the expected red shift[32] due to aggregation of the spheres.

Excitation and emission spectra (Figures 2(b) and 2(c)) were obtained from two different locations on the AuNS gradient substrate corresponding to particle coverages of approximately 15% and 35%, corresponding to well-dispersed and

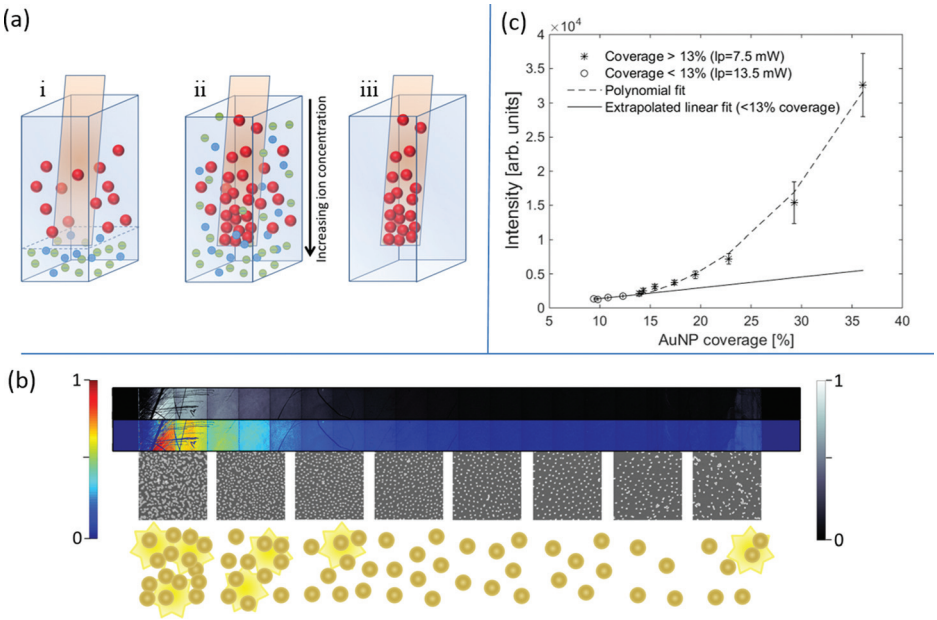

FIG. 1. (a) Schematic illustration of the manufacturing process of the gradient substrates (not to scale). A glass substrate (size: 8.7 × 8.5 mm) (i) modified with APDES is vertically positioned in a solution of AuNSs (d = 10 nm) and low ionic strength. A high ionic strength buffer (ii) is injected from the bottom, whereupon ions diffuse upwards causing an ionic strength gradient, triggering a backfill (iii) of the particles becoming deposited on the surface. (Redrawn with permission from Lundgren *et al.*, Part. Part. Syst. Charact. **31**(2), 209 (2014). Copyright 2014 John Wiley and Sons.) (b) Emission signal (560–680 nm) acquired along the gradient substrate using MPM. A tile of 22 consecutive images scanned across the substrate (field of view: 0.425 × 9.45 mm) is presented in both false color and grayscale. All settings, i.e., excitation wavelength (740 nm), laser power, scan speed, gain, and offset, were kept constant. SEM images are also included (field of view 545 × 545 nm), illustrating the particle distribution at different locations across the substrate. Unintentional scratches on the substrate are observed as irregular dark lines of the emission signal. A conceptual illustration of the correlation between emission and particle distribution is included. (c) Analysis of the emission acquired from three substrates (n = 3) as function of particle coverage. Maximum coverage measured from the SEM images was 37%. Laser power was increased from 7.5 mW to 13.5 mW (measured at back aperture of objective lens) to elevate signal from regions with low coverage (<13%). Included in figure is polynomial ($y = x^3$) and linear fit to demonstrate deviation from linear dependency. Error bars show standard deviation of acquired intensity variation within 5 selected regions corresponding to the same particle coverage.

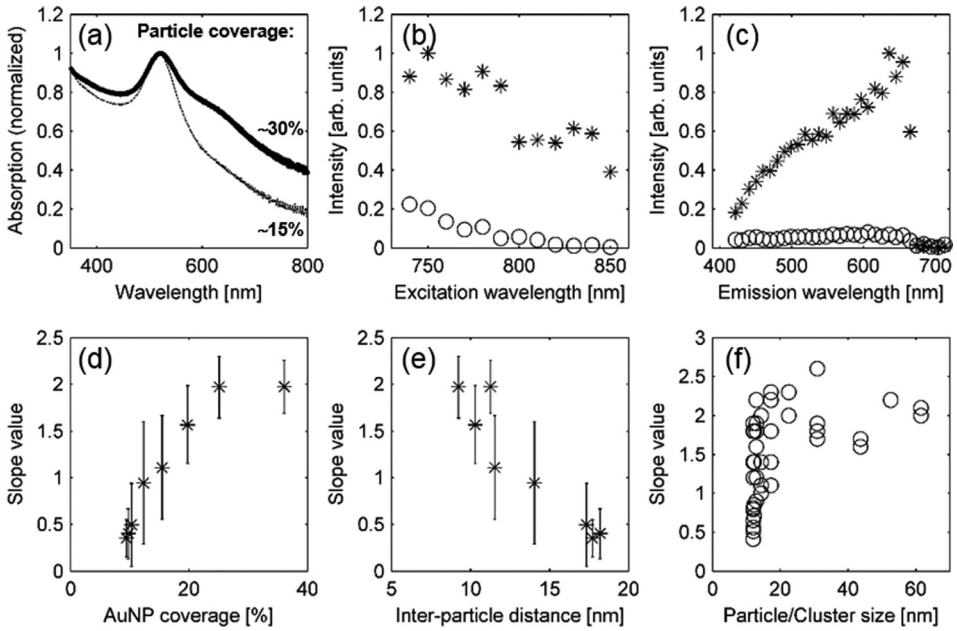

FIG. 2. (a) Absorption spectra obtained from substrate at locations with varying coverage of 10 nm AuNSs. Spectra are normalized with respect to maximum absorption at the plasmon resonance peak (i.e., 520 nm). Multiphoton excitation ((b), emission 560–680 nm) and emission ((c), excitation 740 nm) spectra acquired from the substrate at locations corresponding to 15% (o) and 35% (*) coverage, corresponding to purely well-dispersed and predominantly clustered particles. The drop-off at 670 nm in the emission spectrum (c) corresponds to the cut-off wavelength of the dichroic mirror in the MPM setup. The excitation and emission spectra have been normalized with respect to maximum intensity of emission for clarity. The acquired slope values extracted from the emission intensity as function of laser power plotted as a function of particle coverage (d), the inter-particle distance (e), and average size of particles/clusters (f) for data acquired at different locations along the substrate.

predominantly clustered AuNSs, respectively. Excitation spectra (Figure 2(b)) were acquired by sequentially changing the excitation wavelength in 10 nm increments, detecting the emission in the range of 560–680 nm. The luminescence was found to be strongly dependent on excitation wavelength for the well-dispersed spheres (15% coverage). A flatter excitation spectra was observed at higher particle coverage (i.e., 35%) which implies that the emission signal is less sensitive to the excitation wavelength at such coverages. Emission spectra (Figure 2(c)) were acquired using the spectral detector of the MPM and 740 nm excitation, demonstrating a continuous increase in emission intensity with wavelength for the 35% particle coverage. The sharp drop-off is caused by the cut-off from the dichroic mirror. The general shape of the emission spectrum resembles data from gold nanorods.[12] A wavelength-dependency could not be discerned due to the low signal from the regions with sparsely distributed particles.

To determine the physical origin of the emission, the slope values[30] were investigated by analyzing the dependence of the emitted signal on the laser power. As non-linear dependency was expected for MIL, slope values above one were expected. The average intensity for each examined region of the gradient plate was plotted against the laser power on a logarithmic scale and the slope values were obtained by linear regression using MatLab. In Figures 2(d)–2(f), the calculated slope values from the emission data are presented as function of particle coverage, the inter-particle distance, and cluster size. As shown by the figure, a non-linear dependency corresponding to MIL signal, i.e., a slope value around 2, was only observed from regions of the substrate where the inter-particle distance was measured to be less than around 10 nm (Figure 2(e)). When the inter-particle distance increases, the non-linearity vanishes. This effect is consistent with the fact that enhanced plasmon coupling between closely spaced particles have been confirmed.[33] Furthermore, MIL was only observed when the particles size was increased because of clustering (Figure 2(f)). A size above 20 nm corresponds to clusters of at least two AuNSs. The same low slope value was found in low particle coverage areas of the substrates. The origin of the linear emission, i.e., slope values around 1, can either be attributed to a superposition of the background noise and a weak MIL at the detection limit, or to one-photon induced anti-Stokes emission, which has been reported from gold nanostructures.[34–36] The particles are expected to be heated during the illumination by fs NIR laser light, and thereby become thermally excited. Thus, it is likely that slope values around 1 most likely correspond to anti-Stokes emission.

Interestingly, a decreasing emission signal similar to rapid "photo-bleaching" was observed during the scanning of the plates. This phenomenon is illustrated by Figure 3. The intensity of the emission from the exposed area dropped to 30% of the original signal after exposure, using a laser power of 3 mW, scanning the area for 150 s. The emission in the exposed area recovered to 90% of the original intensity, and repeated exposure using the same light dose resulted in a similar reduction in signal. This result was unexpected as gold nanoparticles are referred to as photostable.[4,37] The effect can possibly be attributed to temporary damping of the plasmon resonance due to creation of a "hot," non-Fermi electronic distribution, which has been reported in pump-probe experiments.[38,39] Another plausible explanation is photo-oxidation caused by stripping electrons from the particles reducing the plasmon resonance.[40] The signal returns as the gold is reduced by the surrounding molecules. The irreversible part of the observed "photo-bleaching" is most

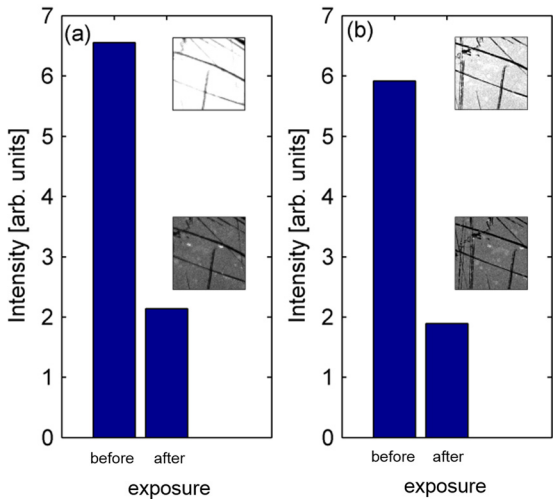

FIG. 3. Luminescence signal as function of laser exposure (740 nm) of high coverage area of the substrate during (a) first exposure and (b) repeated exposure after recovery.

likely attributed photothermal decomposition of the particles. Given the average powers used in the experiment, the pulse energy deposited in the focus can be estimated to 1 pJ. Estimating the focal area of 0.2 μm^2, and given the diameter of the particles is 10 nm, each particle will be exposed to 5 fJ per pulse. The energy required to melt dispersed gold nanorod has been measured to be approx. 60 fJ.[41] Given the pixel dwell time and repetition rate of the laser, each particle will be subject to approx. 200 pulses, causing the total deposited energy per particle during exposure to be well above this melting threshold. Particle melting is thus a possible cause of the irreversible loss of MIL.

The physical principle behind MIL is attributed to a sequential absorption of multiple photons, followed by photoluminescence caused by recombination of conduction band electrons with holes in the *d*-band.[13,34,42] This process is schematically illustrated in Figure 4. During the absorption of the first photon, one electron from the partially filled *sp*-band is excited above the Fermi-level, leaving an electron hole. This intra-band transition is interpreted to be related to the excitations of the plasmon (as will be further discussed below). The hole in the *sp*-band is subsequently filled by an electron that is excited from the *d*-band by the sequential absorption of a second photon and can be considered a single particle excitation. The sequential process creates an excited system, with energy greater than the incoming photon-energy. In competition with other thermalization processes, the excited *d*-hole can decay radiatively giving rise to luminescence.[42,43] When the hole in the *d*-band is recombined with the excited electron in the *sp*-band, a photon with greater energy than that of the single exciting photons is emitted. By changing the pulse length of the exciting photons, the sequential process can be tuned between two-, three-, and four-photon processes.[23] Based on the square power dependence, it is evident that the MIL signal from the aggregated particles in this study is based on a two-photon absorption process.

It is known that clustering of single AuNSs elevates the one-photon plasmonic absorption spectrum in the red region (also observed in our absorption measurements in the shape sensitive region of the spectra, Figure 2(a)). This increased

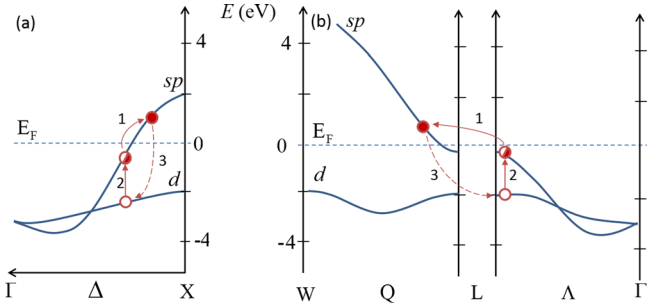

FIG. 4. Schematic diagram of the band structure of Au near the X (a) and L (b) symmetry points, as calculated by Eckardt *et al.*[44] The physical process leading to MIL is conceptually illustrated as a sequential absorption[13,23] of two NIR photons (approx. 1.5 eV). The absorption of the first photon (1) leads to an intra-band indirect transition within the *sp*-band from a conduction electron, leaving behind a hole below the Fermi-level. This hole is then filled by an electron from the *d*-band by absorption of a subsequent photon (2). The bent arrows imply that electronic transitions are coupled to phonon excitations. The luminescence is represented as an inter-band transition occurring when an *sp*-band electron refills the hole in the *d*-band. The dashed arrow indicate that thermalization and scattering might precede transition.[42,43] E_F indicates the Fermi surface. (Band structure redrawn with permission from Eckardt *et al.*, J. Phys. F: Met. Phys. **14**(1), 97 (1984). Copyright 1984 IOP Publishing.)

absorption will in turn contribute to an increased probability for the first plasmon driven intra-band transition and the creation of the first electron hole in the *sp*-band, as illustrated by Figure 4. This is in line with earlier observations,[12,13] demonstrating that the plasmon along the long axis of gold nanorods is resonantly coupled to the photoinduced luminescence. The wavelength dependence observed in the excitation spectra (Figure 2(b)) further supports the conclusion that the MIL is related to excitation of plasmon resonances of the particle aggregates in the NIR region, as the excitation spectra resembles the shape one-photon absorption spectra in this range. This field enhancement and plasmon coupling caused by formation of elongated chain- and rod-like structures will enhance the emission.[15,18,33] The sequential two-photon induced luminescence can be described by[45]

$$\frac{dN_{sp}}{dt} = \sigma_{sp\to sp} N F(t) - \frac{N_{sp}}{\tau_{sp}} - \sigma_{d\to sp} N_{sp} F(t), \quad (1)$$

$$\frac{dN_d}{dt} = \sigma_{d\to sp} N_{sp} F(t) - \frac{N_d}{\tau_d}, \quad (2)$$

N is the electron density in the *sp*-band, N_{sp} and N_d are the densities of holes created below the Fermi-level in the *sp* and *d*–bands, respectively. τ_{sp} and τ_d are the relaxation times of the *sp* and *d*-holes. $F(t)$ is the photon flux and $\sigma_{sp\to sp}$ and $\sigma_{d\to sp}$ represent the cross sections of first and second absorption event. The third term in (1) can be neglected as $N_{sp} \ll N$. Since aggregation and/or clustering of the gold nanospheres will increase the cross section of the first event ($\sigma_{sp\to sp}$) in the NIR region, it follows that more holes are created in the *sp*-band (N_{sp}). Subsequently, the formation of holes in the *d*-band (N_d) will increase according to (2), giving raise to the observed enhancement of MIL signal from the clustered particles.

Thus, our results demonstrate that clustering is crucial in order to observe MIL using MPM. Signal from monomeric spherical particles with diameter below 40 nm should not be expected in far-field MPM mainly because the

one-photon absorption of NIR is too low to allow for the sequential absorption process to take place.[30] This is contradictory to what is implied by other reports.[24–27] A forthcoming study demonstrates that the same effect as discussed herein also applies for particles dispersed in solution (manuscript in preparation). Therefore, despite being a simplistic model, the conceptual insights attained in the present study are highly relevant to understand the underlying physical processes also in more complex systems such as in three dimensions.

It is known that gold nanorods exhibit substantially stronger MIL signal compared to AuNSs.[12,18,19] It has also been earlier implied that aggregating spherical particles exhibit stronger MIL signal compared to individual particles.[14,15] A complete understanding of this process is of importance for novel biomedical applications such as, e.g., optical sensing *in vivo*. Since nanorods have a strong luminescence also when dispersed, they will give rise to a signal despite not being bound to a specific target, leading to a strong background and reduced contrast and signal-to-noise ratio. If instead nanospheres are applied, MIL is only present when particles are clustered and/or aggregated. By choosing a system where aggregation occurs only at a specific physiological condition, this will dramatically improve the signal-to-noise ratio and improve contrast.

Taken together, the results are of importance for future studies, particularly when applying MIL in biomedical applications, as the spherical AuNPs have to be either closely packed or clustered, in order to give rise to MIL signal in a commercial MPM setup. Detection of MIL signal from single 10 nm AuNSs in a biological environment is unlikely. We also report on a "photo-bleaching" effect, possibly attributed to a combination of plasmon damping and photo-oxidation. Future work should be undertaken to investigate AuNSs of other sizes using the same methodology, as well as explore how the clustering can be controlled in a biological environment, e.g., to develop approaches for *in vivo* optical sensing.

The authors would like to thank Anders Lundgren and Timur Shegaiand, Chalmers University of Technology, Danni Wang, Biomedical photonics, University of Gothenburg, for valuable discussions, and Piotr Jedrasik, Chalmers University of Technology, for performing AFM measurements. We acknowledge the Centre for Cellular Imaging, University of Gothenburg, for use of imaging equipment and kind support from the staff. We also thank Cline Scientific AB, for valuable input regarding the substrates. Financial support was obtained from the Swedish Research Council (621-2011-5189) and Marie Curie Initial Training Networks Project CYCLON (No. 237962). We also thank the Centre for Skin Research (SkinResQU), Gothenburg, for use of infrastructure.

[1]R. A. Sperling, P. R. Gil, F. Zhang, M. Zanella, and W. J. Parak, Chem. Soc. Rev. **37**, 1896 (2008).
[2]W. P. Faulk and G. M. Taylor, Immunochemistry **8**, 1081 (1971).
[3]R. Hermann, P. Walther, and M. Müller, Histochem. Cell Biol. **106**(1), 31 (1996).
[4]J. Aaron, N. Nitin, K. Travis, S. Kumar, T. Collier, S. Y. Park, M. José-Yacamán, L. Coghlan, M. Follen, R. Richards-Kortum, and K. Sokolov, J. Biomed. Opt. **12**(3), 034007 (2007).
[5]J. Park, A. Estrada, K. Sharp, K. Sang, J. A. Schwartz, D. K. Smith, C. Coleman, J. D. Payne, B. A. Korgel, A. K. Dunn, and J. W. Tunnell, Opt. Express **16**(3), 1590 (2008).
[6]N. J. Durr, T. Larson, D. K. Smith, B. A. Korgel, K. Sokolov, and A. Ben-Yakar, Nano Lett. **7**(4), 941 (2007).
[7]I. H. El-Sayed, X. Huang, and M. A. El-Sayed, Nano Lett. **5**(5), 829 (2005).
[8]M. B. Dowling, L. Li, J. Park, G. Kumi, A. Nan, H. Ghandehari, J. T. Fourkas, and P. Deshong, Bioconjugate Chem. **21**(11), 1968 (2010).
[9]J. Paoli, M. Smedh, A. M. Wennberg, and M. B. Ericson, J. Invest. Dermatol. **128**(5), 1248 (2008).
[10]E. Dimitrow, M. Ziemer, M. J. Koehler, J. Norgauer, K. Konig, P. Elsner, and M. Kaatz, J. Invest. Dermatol. **129**(7), 1752 (2009).
[11]A. Bouhelier, M. Beversluis, and L. Novotny, Appl. Phys. Lett. **83**(24), 5041 (2003).
[12]H. Wang, T. B. Huff, D. A. Zweifel, W. He, P. S. Low, A. Wei, J.-X. Cheng, and Y. R. Shen, Proc. Natl. Acad. Sci. U. S. A. **102**(44), 15752 (2005).
[13]K. Imura, T. Nagahara, and H. Okamoto, J. Phys. Chem. B **109**, 13214 (2005).
[14]R. A. Farrer, F. L. Butterfield, V. W. Chen, and J. T. Fourkas, Nano Lett. **5**(6), 1139 (2005).
[15]S. Nah, L. Li, and J. T. Fourkas, J. Phys. Chem. A **113**(16), 4416 (2009).
[16]M. I. Stockman, Science **348**(6232), 287 (2015).
[17]G. T. Boyd, Z. H. Yu, and Y. R. Shen, Phys. Rev. B **33**(12), 7923 (1986).
[18]M. B. Mohamed, V. Volkov, S. Link, and M. A. El-Sayed, Chem. Phys. Lett. **317**(6), 517 (2000).
[19]K. Imura, T. Nagahara, and H. Okamoto, J. Am. Chem. Soc. **126**, 12730 (2004).
[20]W. Rechberger, A. Hohenau, A. Leitner, J. R. Krenn, B. Lamprecht, and F. R. Aussenegg, Opt. Commun. **220**(1–3), 137 (2003).
[21]C. Sonnichsen, B. M. Reinhard, J. Liphardt, and A. P. Alivisatos, Nat. Biotechnol. **23**(6), 741 (2005).
[22]Y. Sun and Y. Xia, Anal. Chem. **74**(20), 5297 (2002).
[23]P. Biagioni, D. Brida, J.-S. Huang, J. Kern, L. Duò, B. Hecht, M. Finazzi, and G. Cerullo, Nano Lett. **12**(6), 2941 (2012).
[24]A. Anzalone, M. Gabriel, L. C. Estrada, and E. Gratton, PLoS One **10**(4), e0124975 (2015).
[25]L. C. Estrada and E. Gratton, ChemPhysChem **13**(4), 1087 (2012).
[26]I. Fortunati, V. Weber, E. Giorgetti, and C. Ferrante, J. Phys. Chem. C **118**(41), 24081 (2014).
[27]K. Li and M. Schneider, J. Biomed. Opt. **19**(10), 101505 (2014).
[28]H. Elwing, S. Welin, A. Askendal, U. Nilsson, and I. Lundström, J. Colloid Interface Sci. **119**(1), 203 (1987).
[29]A. Lundgren, M. Hulander, J. Brorsson, M. Hermansson, H. Elwing, O. Andersson, B. Liedberg, and M. Berglin, Part. Part. Syst. Charact. **31**(2), 209 (2014).
[30]See supplementary material at http://dx.doi.org/10.1063/1.4936554 for additional methods, data and discussion.
[31]W. Haiss, N. T. K. Thanh, J. Aveyard, and D. G. Fernig, Anal. Chem. **79**, 4215 (2007).
[32]E. Martinsson, B. Sepulveda, P. Chen, A. Elfwing, B. Liedberg, and D. Aili, Plasmonics **9**, 773 (2014).
[33]J. R. Krenn, A. Dereux, J. C. Weeber, E. Bourillot, Y. Lacroute, J. P. Goudonnet, G. Schider, W. Gotschy, A. Leitner, F. R. Aussenegg, and C. Girard, Phys. Rev. Lett. **82**(12), 2590 (1999).
[34]M. R. Beversluis, A. Bouhelier, and L. Novotny, Phys. Rev. B **68**(11), 115433 (2003).
[35]Y. He, K. Xia, G. Lu, H. Shen, Y. Cheng, Y. C. Liu, K. Shi, Y. F. Xiao, and Q. Gong, Nanoscale **7**(2), 577 (2015).
[36]J. Huang, W. Wang, C. J. Murphy, and D. G. Cahill, Proc. Natl. Acad. Sci. U. S. A. **111**(3), 906 (2014).
[37]C. Sönnichsen and A. P. Alivisatos, Nano Lett. **5**(2), 301 (2005).
[38]T. S. Ahmadi, S. L. Logunov, and M. A. El-Sayed, J. Phys. Chem. **100**(20), 8053 (1996).
[39]M. Perner, P. Bost, U. Lemmer, G. Von Plessen, J. Feldmann, U. Becker, M. Mennig, M. Schmitt, and H. Schmidt, Phys. Rev. Lett. **78**(11), 2192 (1997).
[40]J.-P. Sylvestre, S. Poulin, A. V. Kabashin, E. Sacher, M. Meunier, and J. H. Luong, J. Phys. Chem. B **108**(43), 16864 (2004).
[41]S. Link and M. A. El-Sayed, J. Chem. Phys. **114**(5), 2362 (2001).
[42]P. Biagioni, M. Celebrano, M. Savoini, G. Grancini, D. Brida, S. Mátéfi-Tempfli, M. Mátéfi-Tempfli, L. Duò, B. Hecht, G. Cerullo, and M. Finazzi, Phys. Rev. B **80**(4), 045411 (2009).
[43]A. Mooradian, Phys. Rev. Lett. **22**(5), 185 (1969).
[44]H. Eckardt, L. Fritsche, and J. Noffke, J. Phys. F: Met. Phys. **14**(1), 97 (1984).
[45]P. Biagioni, M. Savoini, J. S. Huang, L. Duò, M. Finazzi, and B. Hecht, Phys. Rev. B: Condens. Matter Mater. Phys. **80**(15), 153409 (2009).